ICMIEE18-109

Boundary Layer Flow of Micropolar Fluid over a Stretching Conical Surface with Magnetic Effect

M. Ali [1], M. A. Alim[2], R. Nasrin[3], Md. Delowar Hossain[4]*
[1, 4] Department of Mathematics, Chittagong University of Engineering & Technology, Chittagong-4349, BANGLADESH
[2, 3] Department of Mathematics, Bangladesh University of Engineering & Technology, Dhaka-1000, BANGLADESH

ABSTRACT
Similarity solution of unsteady forced convection magnetohydrodynamic boundary layer flow and heat transfer over a porous stretching cone are analyzed. The governing partial differential equations are transformed into ordinary differential equations by using local similarity transformations. The transformed equations are solved numerically subject to the boundary conditions by using Nachtsheim-Swigert iteration technique along with the 4th order Runge-Kutta integration scheme. The numerical results are checked against previously published work for special cases of the problem in order to access the accuracy of the numerical method and found to be in good agreement. The results indicates that the fluid velocity decreases for increasing values of magnetic parameter, porosity parameter and unsteadiness parameter but the reverse results arises for pressure gradient parameter, material parameter and stretching ratio parameter. The heat transfer rate decreases for increasing values of stretching ratio parameter, material parameter, pressure gradient parameter but increases for magnetic parameter, unsteadiness parameter, porosity parameter, Prandtl number and wall temperature parameter. The numerical results are presented graphically and also in tabular form.

Keywords: MHD, microrotation, pressure gradient, stretching.

1. Introduction

The micropolar fluids are fluids which contain microstructure that can undergo rotation. Physically, it represent fluids consisting of randomly oriented particles suspended in a viscous medium. The presence of this type of fluid can affect the hydrodynamic of the flows so that it can be distinctly non- Newtonian. The boundary layer flow of micropolar fluid driven by a continuous stretching surface are important in a number of industrial engineering processes such as colloidal suspensions, the aerodynamic extrusion of plastic sheets, annealing and thinning of copper wires, cooling of metallic plate in a bath, animal blood, body fluids, fluid flowing in brain and so forth. The theory of micropolar fluids was originally formulated by Eringen [1] by taking the local effects arising from the microstructure and the intrinsic motion of the fluid into the account. After that, Adekeye et al. [2] identified that a strong flow circulation arises at particular value of Grashof number and heat transfer rate is significant at certain interval of inclination. Hussein et al.[3] shown that the solid volume fraction has a significant influence on stream function and heat transfer, depending on the value of Hartmann and Rayleigh numbers. Ahmed et al.[4] observed that the skin friction coefficient decreases as the Reynolds number and the suction/injection parameter increases, while the local Nusselt number increases as the Reynolds number and the suction/injection parameter increases. Reddy [5] obtained that the momentum boundary layer thickness is elevated whereas thermal boundary layer thickness is decelerates with the higher values of nanoparticle volume fraction, Norfarahanim [6] discussed Marangoni boundary layer flow in micropolar fluid with suction/injection, Siva Reddy [7] analyzed the heat and mass transfer on the MHD flow of micropolar fluid in the presence of viscous dissipation and chemical reaction, Mostafa et al.[8] studied the MHD flow and heat transfer of a micropolar fluid over a stretching surface with heat generation and slip velocity, Ali et al. [9] studied the similarity solution of MHD free convection heat and mass transfer flow over a porous medium in a rotating system with hall current and heat generation, Ishak et al. [10] discussed magnetohydrodynamic (MHD) flow of a micropolar fluid towards a stagnation point on a vertical surface and found that the micropolar fluid delays the boundary layer separation, Das [11] studied the influence of thermophoresis and chemical reaction on MHD micropolar fluid flow with variable fluid properties and found that in presence of different physical effects can be modified the flow, heat and mass transfer, Bhattacharyya et al. [12] examined the effects of thermal radiation on micropolar fluid flow and heat transfer over a porous shrinking sheet, Redha et al. [13] analyzed the thermal radiation effect on heat and mass transfer in steady laminar boundary layer flow of an incompressible viscous micropolar fluid over a vertical flat plate, in presence of magnetic field, Mohanty et al. [14] studied the effect of micropolar fluid over a stretching sheet through porous media on heat and mass transfer. Recently, Reddy [15] investigated the influence of Soret and Dufour effects on MHD heat and mass transfer flow of a micropolar fluid with thermophoresis particle deposition. Siva Gopal [16] analyzed the effect of Soret and Dufour on unsteady convective heat and mass transfer flow of a micropolar fluid through porous medium past a permeable

* Corresponding author. Mobile: +88-01713109929
E-mail addresses: ali.mehidi93@gmail.com

stretching sheet. The aim of the present work is to investigate the unsteady flow and heat transfer of an electrically conducting micropolar fluid over a stretching cone with uniform transverse magnetic field. The flow is subjected to a transverse magnetic field of strength B_0 which is assumed to be applied in the positive y –direction and normal to the flow direction.

2. Geometry of the present problem

Let us consider the two dimensional unsteady forced convection laminar flow over a stretching cone. The flow is supposed to be electrically conducting. The coordinate system is considered in such a way that x-axis coincides with the surface of the cone, and y-axis is perpendicular to it. A transverse magnetic field of strength B_0 is applied orthogonal to the surface of the cone as depicted in Fig. A. Suppose that β is the half angle of the cone, r is the radius of the cone. The temperature near the surface is considered as $T_w = T_\infty + \frac{ax^s}{1- ct}$, where a is constant, s is the wall temperature parameter, T_∞ is the free stream temperature. We assume that the velocity of a point on a cone is proportional to its distance from the leading edge.

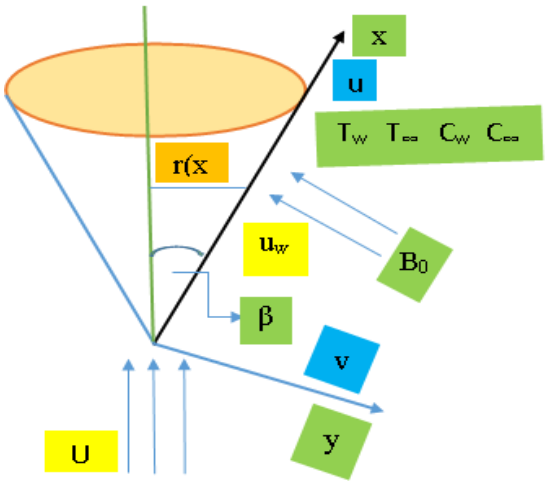

Figure A: Physical model and coordinate system

3. Governing equations and similarity solution

Under the above assumptions and usual boundary layer approximation, the dimensional governing equations of continuity, momentum, microrotation, and energy are:

Equation of continuity:

$$\frac{\partial(ru)}{\partial x} + \frac{\partial(rv)}{\partial y} = 0 \qquad (1)$$

Momentum equation:

$$\frac{\partial u}{\partial t} + u\frac{\partial u}{\partial x} + v\frac{\partial u}{\partial y} = U\frac{dU}{dx} + \frac{dU}{dt} + \left(\frac{\nu + \chi}{\rho}\right)\frac{\partial^2 u}{\partial y^2} + \frac{\chi}{\rho}\frac{\partial N}{\partial y} - \left(\frac{\sigma B_0^2}{\rho} + \frac{\nu}{k}\right)(u - U) \qquad (2)$$

Angular momentum equation:

$$\frac{\partial N}{\partial t} + u\frac{\partial N}{\partial x} + v\frac{\partial N}{\partial y} = -\frac{\chi}{\rho j}\left(2N + \frac{\partial u}{\partial y}\right) + \frac{\gamma}{\rho j}\frac{\partial^2 N}{\partial y^2} \qquad (3)$$

Energy equation:

$$\frac{\partial T}{\partial t} + u\frac{\partial T}{\partial x} + v\frac{\partial T}{\partial y} = \frac{\kappa}{\rho c_p}\frac{\partial^2 T}{\partial y^2} \qquad (4)$$

When microrotation parameter R = 0, we obtain N = 0 which represents no-spin condition i.e. the microelements in a concentrated particle flow-close to the wall are not able to rotate. Again, the constant R is varies in the range of $0 \le R \le 1$. According to Guram and Smith [17], for strong concentration R = 0 and this indicates N = 0, it describes the microelements nearby the wall surface are unable to rotate. While N = 0.5 denoted for weak concentration which signified the disappearance of the anti-symmetric part of the stress tensor. By following the recent work we assuming that $\gamma = \left(\mu + \frac{\chi}{2}\right)j = \mu\left(1 + \frac{K}{2}\right)j$, $K = \frac{\chi}{\mu}$ is the micropolar parameter or material parameter. The Newtonian kinematic viscosity is now supplemented by the Eringen micropolar vortex viscosity, χ. In the present work, we assume that the micro-inertia per unit mass j is constant.

The boundary conditions of the above equations are as follows:

$$u = \frac{ax^m}{1- ct}, v = 0, N = -R\frac{\partial u}{\partial y}, T = T_w \text{ at } y = 0$$

$$u \to U = \frac{bx^m}{1- ct}, N \to 0, T \to T_w \text{ as } y \to \infty$$

The governing partial differential equations are transformed into ordinary differential equations by applying local similarity transformation such as:

$$\eta = y\sqrt{\frac{u}{2\nu x(1-ct)}},\ N = u\sqrt{\frac{u}{2\nu x(1-ct)}}H(\eta)$$

$$\psi = \sqrt{\frac{2\nu ux}{(1-ct)}}(1+n)f(\eta),$$

$$ur = \frac{\partial \psi}{\partial y}, vr = -\frac{\partial \psi}{\partial x}, \theta(\eta) = \frac{T-T_\infty}{T_w-T_\infty}$$

Using this dimensionless quantities, the governing equations together with the boundary conditions are reduced to a set of ordinary differential equations so that the numerical solutions can be calculated easily.

$$(1+K)f''' + \left(\frac{1+m}{2}\right)ff'' + m(1-f'^2) + KH' + M(1-f') + 2A\left(1-f'-\frac{1}{2}\eta f''\right) = 0 \quad (6)$$

$$\left(1+\frac{K}{2}\right)H'' + \left(\frac{1+m}{2}\right)fH' + \frac{1-m}{2}f'H - \frac{2K\zeta}{\mathrm{Re}}(2H+f'') - A\left(H+\frac{1}{2}\eta H'\right) = 0 \quad (7)$$

$$\theta'' + \mathrm{Pr}(1+n)f\theta' - \frac{2\mathrm{Pr}sf\theta}{1+m} - \frac{2A}{1+m}\left(\theta+\frac{1}{2}\eta\theta'\right) = 0 \quad (8)$$

The transform boundary conditions are:

$$f(0)=0, f'(0)=1, H(0)=-\frac{1}{2}f''(0), \theta=1 \text{ at } \eta=0$$

$$f'(\infty)\to\lambda, H(\infty)\to 0, \theta\to 0 \text{ as } \eta\to\infty$$

Where η_∞ is the value of η at which boundary conditions are achieved, the prime denotes differentiation with respect to η and also

$$K = \frac{\kappa}{\rho\nu}, K^* = \frac{2\nu x}{ku} A = \frac{c}{ax^{m-1}}, \lambda = \frac{b}{a},$$

$$\mathrm{Pr} = \frac{\nu}{\alpha}, M = \frac{\sigma B_0^2 x}{\rho u}, \mathrm{Re} = \frac{ux}{\nu}, \zeta = \frac{x^2}{j}$$

are the material parameter, porosity parameter, unsteadiness parameter, stretching ratio, Prandtl number, magnetic parameter, Reynolds number, microinertia density constant respectively.

4. Results and discussion

The Numerical calculation of linear velocity, angular velocity, and temperature for different values of dimensionless parameters are carried out. For the purpose of our simulation we have chosen M = 0.3, m = 0.2, K = 0.4, K* = 0.4, λ = 0.1, A = 0.22, Re = 100, and Pr = 1.0 throughout the calculation while the parameters are varied over range as shown in the figures. Fig.1 clearly shows that the effect of magnetic field is more prominent at the point of peak value, because the presence of M in an electrically conducting fluid produces a resistive force against the flow which is known as drag force and it is prominent at the peak point. As a result linear velocity profiles decreases. Similar result arises for porosity parameter that are displayed in Fig.6. The fluid of linear velocity increases for increasing values of pressure gradient, stretching ratio and material parameter which have depicted in Fig.2, Fig.3 and Fig.4. From Fig. 5 it is observed that the linear velocity decreases up to certain values of eta and then increases. The angular velocity decreases for increasing values of magnetic parameter, porosity and unsteady parameter which have depicted in Fig.7, Fig.11 and Fig.12. From Fig.9 and Fig.10 it is observed that the angular velocity increases for increasing values of stretching ratio and material parameter. From Fig. 8 it is observed that the microrotation decreases up to certain values of eta and then increases. The temperature decreases for increasing values of magnetic parameter, material parameter, unsteady parameter, porosity parameter, Prandtl number and wall temperature parameter which have depicted in Fig. 13 and Fig.16 – Fig.20 but the reverse result arises only for pressure gradient parameter and stretching ratio parameter that have displayed in Fig. 14 and Fig. 15. Further the heat transfer rate has compared with Mohammadi et al.[18] for various values of m with M = K = K* = A = λ = 0. The results have shown in Table 1and it is observed that the present results and those of [18] are almost similar.

Table 1: Comparison of local skin friction $f''(0)$ for different values of m Mohammadi et al.[18]

	Mohammadi *et al.*	Present results
m	$f''(0)$	$f''(0)$
0.0	0.469589	0.46964
1/11	-	0.65500
1/3	0.927601	0.92768
1.0	1.232587	1.232587

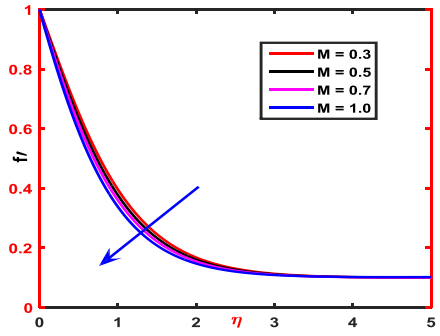

Fig.1. Velocity profiles for magnetic parameter

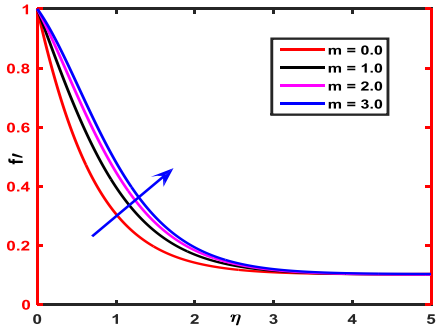

Fig.2. Velocity profiles for pressure gradient

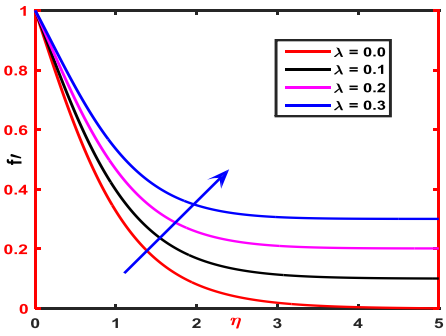

Fig.3. Velocity profiles for stretching ratio

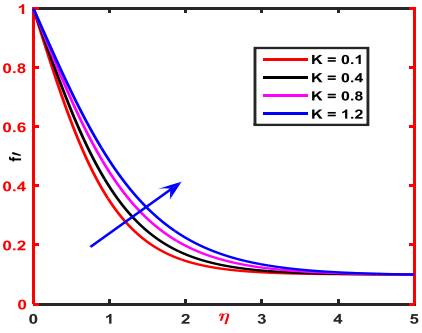

Fig.4. Velocity profiles for material parameter

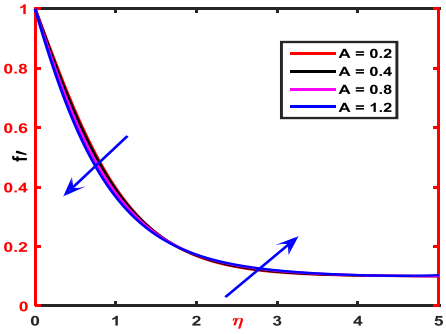

Fig.5. Velocity profiles for unsteady parameter

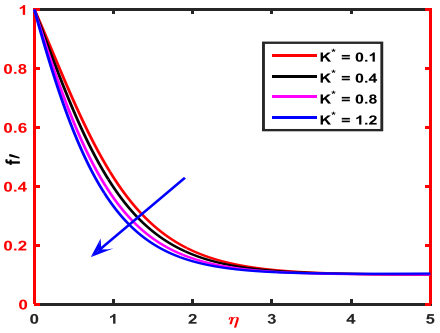

Fig.6. Velocity profiles for porosity parameter

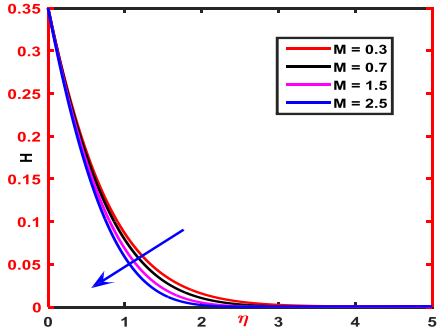

Fig.7. Angular velocity for magnetic parameter

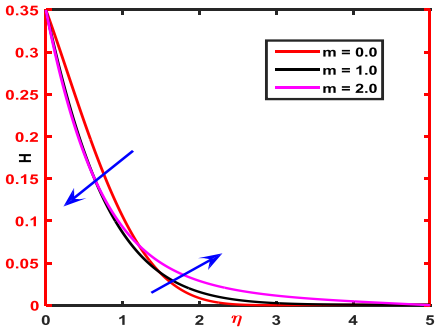

Fig.8. Angular velocity for pressure gradient parameter

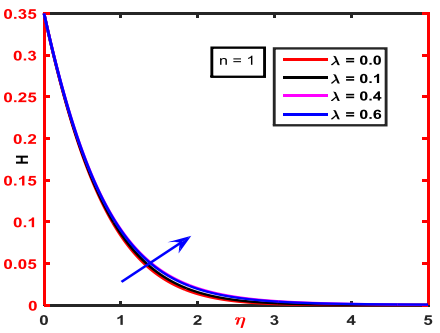

Fig.9. Angular velocity for stretching ratio parameter

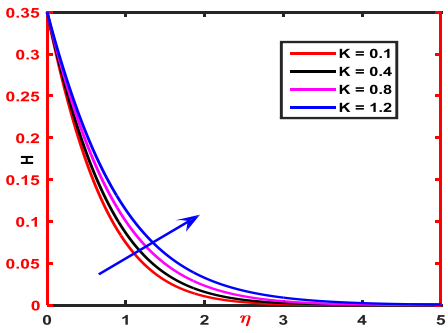

Fig.10. Angular velocity for material parameter

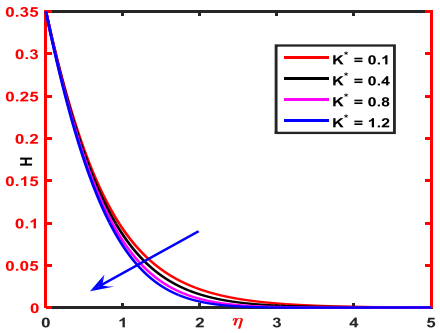

Fig.11. Angular velocity for porosity parameter

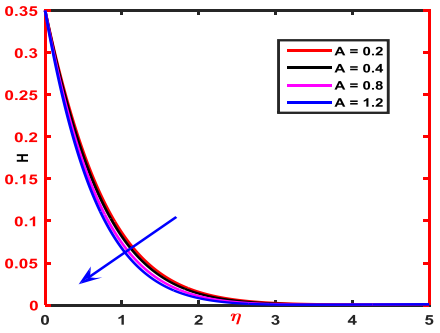

Fig.12. Angular velocity for unsteady parameter

* Corresponding author. Mobile: +88-01713109929
E-mail addresses: ali.mehidi93@gmail.com

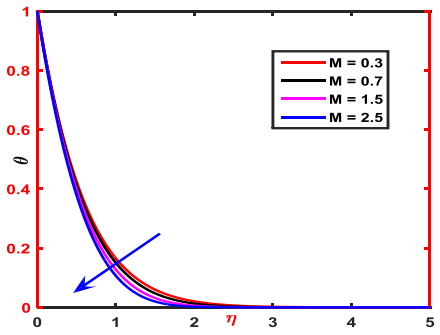

Fig.13. Temperature profiles for magnetic parameter

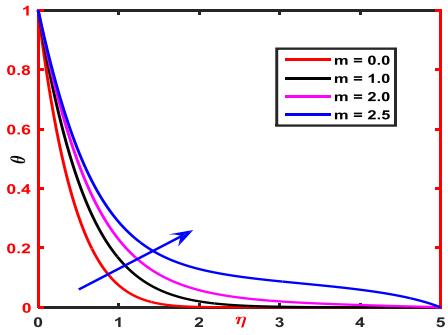

Fig.14. Temperature profiles for pressure gradient parameter

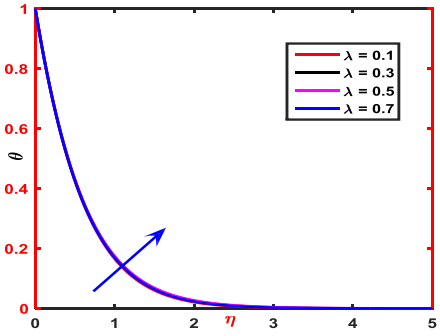

Fig.15. Temperature profiles for stretching ratio parameter

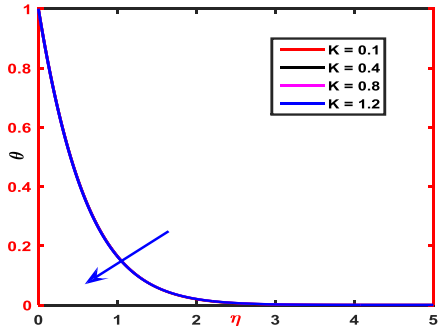

Fig.16. Temperature profiles for material parameter

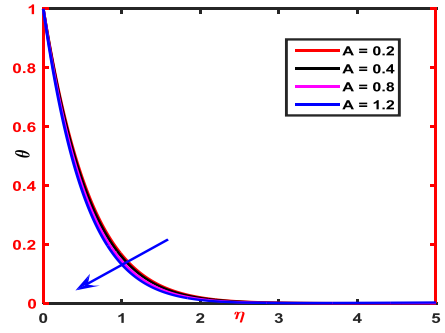

Fig.17. Temperature profiles for unsteady parameter

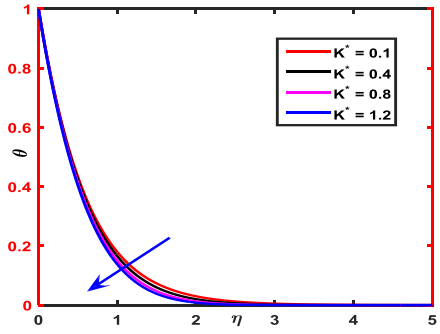

Fig.18. Temperature profiles for porosity parameter

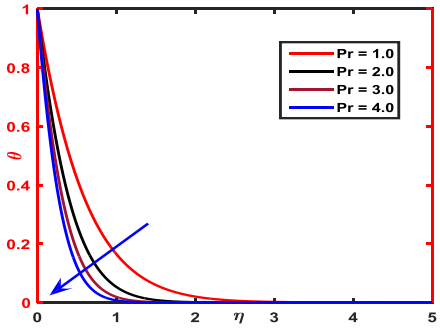

Fig.19. Temperature profiles for Prandtl number

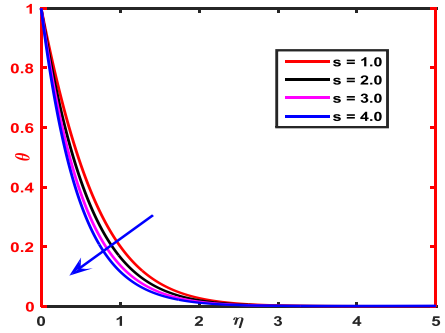

Fig.20. Temperature profiles for wall temperature parameter

5. Conclusions

The conclusions of the present problem are as follows:

- The fluid velocity within the boundary layer are decreases with the increasing values of magnetic parameter and porosity parameter but the reverse trend arises in case of pressure gradient, stretching ratio and material parameter. The fluid velocity decreases up to a certain values of eta and then increases for increasing values of unsteady parameter.
- The angular velocity are decreases for increasing values of magnetic parameter, porosity parameter and unsteady parameter but increases for the increasing values of stretching ratio and material parameter. The angular velocity decreases up to a certain values of eta and then increases for pressure gradient parameter.
- The heat transfer rate increases for increasing values of magnetic parameter, wall temperature parameter, material parameter, Prandtl number, porosity parameter and unsteady parameter but the rate decreases only for stretching ratio and pressure gradient parameter.

NOMENCLATURE

MHD megnetohydrodynamic

c_p specific heat at constant pressure, $Jkg^{-1}K^{-1}$

κ thermal conductivity, $w\ m^{-1}K^{-1}$

β semi vertical angle, degree

g acceleration due to gravity, ms^{-2}
σ electrical conductivity, sm^{-1}
K^* permeability of the porous medium
K material parameter
μ coefficient of viscosity, kg $m^{-1}s^{-1}$
ν kinematics viscosity, m^2s^{-1}
ρ fluid density, kg m^{-3}
B_0 magnetic field intensity, Am^{-1}
u velocity component along x axis, ms^{-1}
v velocity component along y axis, ms^{-1}
a stream velocity constant
b free stream velocity constant
c unsteady constant
A unsteady parameter
η similarity variable
f dimensionless stream function
H microrotation
m pressure gradient
T fluid temperature, k^{-1}
T_w plate temperature, k^{-1}
T_∞ free stream temperature
ψ stream function

REFERENCES

[1] A. C. Eringen, Theory of micropolar fluids, *J. Math. Mech.*, vol. 16, pp. 1–16, (1966).

[2] T. Adekeye, I. Adegun, P. Okekunle, A. K. Hussein, Oyedepo S., Adetiba E. and Fayomi O., Numerical analysis of the effects of selected geometrical parameters and fluid properties on MHD natural convection flow in an inclined elliptic porous enclosure with localized heating, *Heat Transfer-Asian Research*, Vol. 46, pp. 261-293 (2017).

[3] S. Ahmed, A. K. Hussein, H. Mohammed, and S. Sivasankaran, Boundary layer flow and heat transfer due to permeable stretching tube in the presence of heat source/sink utilizing nanofluids, *Applied Mathematics and Computation*, Vol. 238, pp. 149-162 (2014).

[4] S. Ahmed, A. K. Hussein, H. Mohammed, I. Adegun, X. Zhang, L. Kolsi, A. Hasanpour, and S. Sivasankaran, Viscous dissipation and radiation effects on MHD natural convection in a square enclosure filled with a porous medium, *Nuclear Engineering and Design*, Vol. 266, pp. 34-42 (2014).

[5] S. Reddy and A. J. Chamkha, Heat and mass transfer characteristics of MHD three-dimensional flow over a stretching sheet filled with water-based alumina nanofluid, *In. J. Numer. Methods Heat and Fluid Flow* , January 2018.

[6] N. M. Ariffin, Norihan M. Arifin, and N. Bachok, Marangoni boundary layer flow in micropolar fluid with suction/injection, *AIP Conference Proceedings*, Vol. 1795, (2017).

[7] S. R. Sheri and M. Shamshuddin, Heat and mass transfer on the MHD flow of micropolar fluid in the presence of viscous dissipation and chemical reaction, *Procedia Engineering*, Vol. 127, pp. 885 – 892, (2015).

[8] A. A. Mostafa Mahmoud, S. Waheed, MHD flow and heat transfer of a micropolar fluid over a stretching surface with heat generation and slip velocity, *Journal of the Egyptian Mathematical Society*, Vol. 20, pp. 20–27, (2012).

[9] M. Ali, M. A. Alam and M. A. Alim, MHD free convection heat and mass transfer flow through a porous medium in a rotating system with hall current and heat generation, IEEE Xplore Digital Library, pp. 404 – 408, (2014).

[10] A. Ishak, R. Nazar, and I. Pop, Magnetohydrodynamic (MHD) flow of a micropolar fluid towards a stagnation point on a vertical surface,*Comput. Math. Appl.*, vol. 56, pp. 3188-3194, (2008).

[11] K. Das, Influence of thermophoresis and chemical reaction on MHD micropolar fluid flow with variable fluid properties, *Int. J. Heat Mass Transfer*, vol. 55, pp. 7166–7174, (2012).

[12] Bhattacharyya, S. Mukhopadhyay, G. C. Layek and I. Pop, Effects of thermal radiation on micropolar fluid flow and heat transfer over a porous shrinking sheet, *Int. J. Heat Mass Transfer*, vol. 55, pp. 2945–2952, (2012).

[13] A. Redha, M. N. Bouaziz and S. Hanini, Numerical study of micropolar fluid flow heat and mass transfer over vertical plate: effects of thermal radiation, Sci. Tech., Vol. 41, pp.15-22, (2015).

[14] B. Mohanty, S. R. Mishra, and H. B. Pattanayak, Numerical investigation on heat and mass transfer effect of micropolar fluid over a stretching sheet through porous media, *Alexandria Eng. J*., vol. 54, pp. 223–232, (2015).

[15] R. Sudarsan, and A. J. Chamkha, Soret and Dufour effects on MHD heat and mass transfer flow of a micropolar fluid with thermophoresis particle deposition, *J. Naval Arch. Marine Eng.*, vol. 13, pp. 39-50, (2016).

[16] S. Gopal, and P. Siva, Unsteady hydromagnetic heat and mass transfer flow of a micropolar fluid past a stretching sheet with Thermo-Diffusion and Diffusion-Thermo effects, *Int. J. Comput. Appl.*, Vol. 7, pp. 81-97, (2017).

[17] G. S. Guram and A.C. Smith, Stagnation Flows of Micropolar Fluids with Strong and Weak Interactions, Computers and Mathematics in Applications Vol.6, pp. 213-233, (1980).

[18] F. Mohammadi, M. M. Hosseini, A. Dehgahn, F. M. Maalek Ghaini, Numerical Solutions of Falkner-Skan Equation with Heat Transfer, *Studies in Nonlinear Science*, Vol. 3, pp. 86-93,(2012).